Conformational Studies on a Diastereoisomeric Pair of Tricyclic Nonclassical Cannabinoids by NMR Spectroscopy and Computer Molecular Modeling

Xiang-Qun Xie,[†,‡] Spiro Pavlopoulos,[§] C. M. DiMeglio,[∥] and Alexandros Makriyannis*[,†,‡,§]

Institute of Materials Science, School of Pharmacy, The University of Connecticut, Storrs, Connecticut 06269, The Francis Bitter National Magnet Laboratory, Massachusetts Institute of Technology, Cambridge, Massachusetts 02139, and Sterling Chemistry Building, Yale University, New Haven, Connecticut 06520

Received June 10, 1996[⊗]

Among the nonclassical cannabinoids, CP-55,244 (**4**), which incorporates an axial 14β-hydroxymethyl group, is pharmacologically 30 times more potent than its prototype CP-47,497 (**2**) and 300 times more potent than Δ^9-THC (**1**). It has a high degree of stereoselectivity (about 120:1) with respect to its diastereoisomer, CP-97,587 (**5**), which differs structurally by having the 14-hydroxymethyl group equatorial. Conformational studies of **4** and **5** were carried out using 2D NMR spectroscopy and molecular modeling in order to define and compare the similarities and differences between them. Specific structural features of interest are the conformation of the 1′,1′-dimethylheptyl (DMH) side chain, the conformation of the cyclohexyl rings, the orientation of the phenolic ring (A ring) relative to the cyclohexyl ring (C ring), and the orientation of the hydroxymethyl group as well as the formation of intramolecular hydrogen bonding. Our results show that the conformations of the phenolic hydroxyl (Ph-OH) and DMH side chain for **4** are similar to those of **2**. The proton of the phenolic hydroxyl is pointing away from the C ring while the DMH chain randomly adopts one of four dynamically averaged conformers in which it is almost perpendicular to the plane of the aromatic ring. The relative orientation of the A and C rings is such that the two rings interconvert between two low-energy conformations. Compound **5** prefers the conformer with the Ph-OH pointing toward the α-face of the cyclohexyl ring, while for **4**, there is an increased preference for the conformer where the Ph-OH is directed toward the β face. This may be due to intramolecular H-bonding between the Ph-OH and the axial 14β-hydroxymethyl group of **4** that stabilizes this conformation. Hydrogen bonding between the Ph-OH and the equatorial 14α-hydroxymethyl of **5** was not detected. Thus, the orientation of the aliphatic hydroxyl group with respect to the D ring in **4** and **5** may play an important role with regard to the pharmacophoric requirements of the two analogs for the cannabinoid receptor and provide an explanation for the observed differences in their biological properties.

Introduction

Since the main biologically active constituent in marijuana (*Cannabis sativa*) was identified in the 1960s[1] as (−)-Δ^9-tetrahydrocannabinoid (**1**), the structures of cannabinoids have experienced a significant evolution toward more potent synthetic analogs (Figure 1).[1−5] A series of new cannabinoid compounds possessing only the most essential pharmacophores were designed and synthesized with the aim of obtaining novel analgesic agents that are devoid of the psychotropic properties of marijuana. The essential pharmacophoric requirements for cannabimimetic activity include the phenolic OH (Ph-OH), the dimethylheptyl side chain (DMH), and the cyclohexyl ring (C ring)[6] (Figure 1). Those analogs were named *nonclassical cannabinoids* (NCCs) since they deviate structurally from the naturally occurring tricyclic tetrahydrocannabinols by the absence of a tetrahydropyran ring.[4,6] Figure 1 shows several selected NCCs: **2** (CP-47,497) is the NCC prototype with the most simplified structure; **3** (CP-55,940) is an important ligand that was used in the identification of the cannabinoid receptor; **4** (CP-55,244) and **5** (CP-97,587) are two diastereoisomeric NCCs possessing widely different cannabimimetic potencies. In earlier publications we reported the conformational properties of **2** and **3**.[7a,b] The focus of the present communication is now the structurally more elaborate diastereoisomers, 4-[4-(1,1-dimethylheptyl)-2-hydroxyphenyl]perhydro-2α,6β-dihydroxynaphthalene (**4**) and 4-[4-(1,1-dimethylheptyl)-2-hydroxyphenyl]perhydro-2α,6α-dihydroxynaphthalene (**5**). For ease of discussion these compounds have been numbered as shown in Figure 1. Unlike **2**[7a] and **3**,[7b] the two diastereomeric NCCs presented in this paper are tricyclic compounds. The presence of a third ring (or D ring) in **4** and **5** results in two analogs in which the 14-hydroxymethyl (or southern hydroxymethyl) group is more spatially restricted as compared to the hydroxypropyl group of **3** (Figure 1).

Compound **4** has an axial or 14β-hydroxymethyl group while **5** incorporates an equatorial or 14α-hydroxymethyl. Pharmacologically, **4** is 30 times more potent than its prototype **2** and 300 times more potent than **1**.[8,9] It has a high degree of stereoselectivity, being approximately 120 times more potent than its diastereoisomer, **5**. The different orientation assumed by the

[†] Institute of Materials Science, The University of Connecticut.
[‡] The Francis Bitter National Magnet Laboratory, MIT.
[§] School of Pharmacy, The University of Connecticut.
[∥] Sterling Chemistry Building, Yale University.
[⊗] Abstract published in *Advance ACS Abstracts,* December 1, 1997.

S0022-2623(96)00410-4 CCC: $15.00
Published on Web 01/15/1998

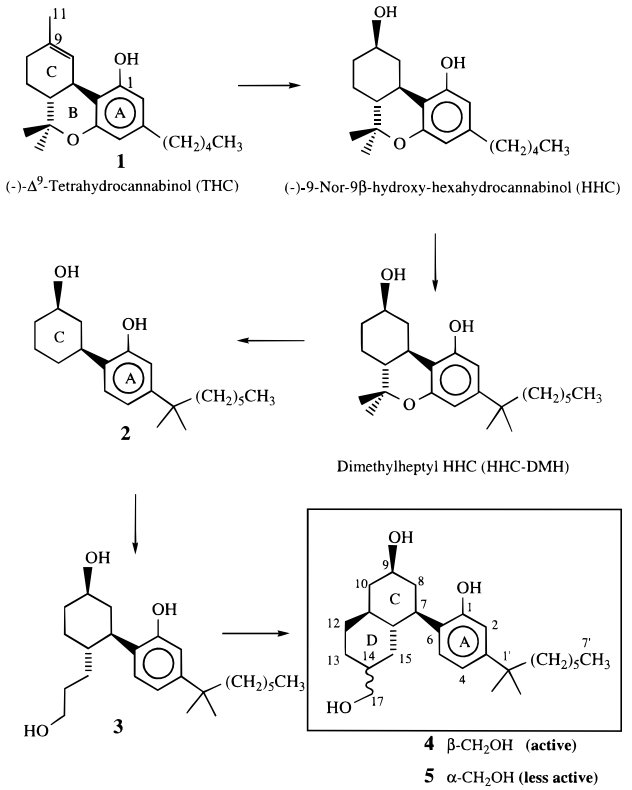

Figure 1. Evolution in cannabinoid structures with progressively enhanced potencies from naturally occurring Δ^9-THC toward a more potent and stereoselective synthetic analog (**4**).

aliphatic hydroxyl group with respect to the D ring in **4** and **5** may be critical in determining the pharmacophoric requirements in the cannabinoid receptor and provide an explanation for the observed differences in their biological properties.

In this paper, we report the conformational properties of the tricyclic nonclassical cannabinoids **4** and **5** as determined by NMR spectroscopy and computational analysis. Specifically, the conformation of the cyclohexyl rings C and D, the position of the A ring relative to the C ring, the orientation of Ph-OH, and the orientations of the DMH side chain and of the solution aliphatic hydroxyl group are examined in an attempt to shed light on the difference in activity between these two diastereoisomers.

Materials and Methods

Materials. Nonclassical cannabinoids were kindly provided to us by Pfizer Central Research (Groton, CT), Deuterated chloroform ($CDCl_3$) and tetramethylsilane (TMS) were purchased from Aldrich Chemical Co. (Milwakee, WI), and deuterated dimethyl sulfoxide (DMSO) containing 1% TMS from Cambridge Isotope Laboratories. NMR samples were prepared as 0.02 M, thoroughly degassed by the freeze−thaw method, and sealed in high-quality 5 mm NMR tubes (no. 528, Wilmad Glass Co., Buena, NJ). TMS was used as an internal chemical shift reference in all samples.

NMR Spectra. High-resolution ^{1}H NMR spectra were collected on a Bruker AVANCE DMX500 spectrometer with a 5 mm inverse detection triple resonance probe and a BVT-2000 temperature controller. 1D ^{1}H NMR spectra were obtained with a spectral width of 4921.26 Hz and 32K data points at temperatures of 263−333 K for $CDCl_3$ spectra and at 298 K for DMSO spectra. Double-quantum-filtered COSY[10] (DQFCOSY), NOESY,[11] and ROESY[12] spectra were recorded with a spectral width of 4921.26 Hz and 2K data points in the F2 dimension for 512 transients. The F1 dimension was zero-filled to 2K data points prior to 2D Fourier transformation to yield a 2K × 2K data matrix. 2D spectra of $CDCl_3$ samples were acquired at temperatures ranging from 263 to 333 K and for DMSO spectra at 298 K. NOESY and ROESY spectra were acquired with mixing times of 100, 300, and 500 ms. The simulations of the 1D ^{1}H NMR spectra of **4** and **5** corresponding to the bicyclohexyl ring and hydroxymethyl chain were performed using an ASPECT3000 computer and the LAOCOON-based PANIC software[13] from the Bruker computer program library, and as we have described elsewhere.[7a,b,14] The spectral parameters defining the spin system comprise chemical shifts and scalar coupling constants (J coupling) that were estimated from 2D phase-sensitive COSY spectra. These values were used as the starting point for an iterative simulation of subspectra. The refined ^3J values were then used to calculated the dihedral angles from the Karplus equation[15] as described later.

Computer Molecular Modeling. The conformational properties of **4** and **5** were studied using computational approaches described by us in earlier publications.[7a,b] Molecular modeling calculations were carried out by using the InsightII/DISCOVER program package[16] on a Silicon Graphics 4D/70GT workstation. Calculations were carried out using AMBER[17] and CVFF[18] force fields with similar results obtained in each case. The atomic charges were calculated using the semiquantum molecular orbital method MOPAC (AM1).[19] Bond rotary searches (or dihedral drive technique) were performed to calculate energy barriers and define preferred angles. Normally, typical intervals of 5° were used for single bond rotation, and 10° for two-bond rotation. Energy barriers, calculated by simply rotating about a bond while maintaining the remaining bonds and angles rigid, can be erroneously high due to van der Waals overlapping. To avoid this problem and relax the whole molecule, energy minimization was carried out, during which an additional torsion force (200 kcal/rad^2) was applied in order to restrain the dihedral angle at the new value to which it had been rotated. The conformational search was performed following a method similar to that used for calculating energy barriers, except that the two dihedral angles were rotated in an orderly fashion.

Results

Computational Results. The results of the conformational search for the DMH side chain are similar to those reported earlier for **2** and **3**, with four equienergetic conformations. In order to simplify our simulations, the dihedral angles ϕ_3 (C2−C3−C1′−C2′) and ϕ_4 (C3−C1′−C2′−C3′) of the DMH groups were arbitrarily set to −56° and −58°, respectively, according to one of the four conformations.[7a,b]

One-bond drive calculations were performed to determine the rotational energy barriers of the C6−C7 bond between the A and C rings. Upon incrementally rotating around the C6−C7 bond, the energy gradually increases up to the point where the two rings are almost "coplanar" (ϕ_1 (C5−C6−C7−C8) = 30°). Two energy minima were detected corresponding to conformations in which the plane of the aromatic ring was perpendicualr to that of the cyclohexyl rings with the Ph-OH facing either the α or β face of the cyclohexyl rings (ϕ_1 = 63° and ϕ_1 = −115°, respectively). The energy difference between the two minima is 0.7 kcal mol^{-1}, and the calculated rotational energy barrier between the two low-energy conformations is 20.5 kcal mol^{-1} for **4** and 21.2 kcal mol^{-1} for **5**.

Two-bond rotary searches were conducted to investigate the conformational properties of the hydroxymethyl group (or southern OH) for both molecules. Figure 2 shows an energy contour map for **5** as a function of the

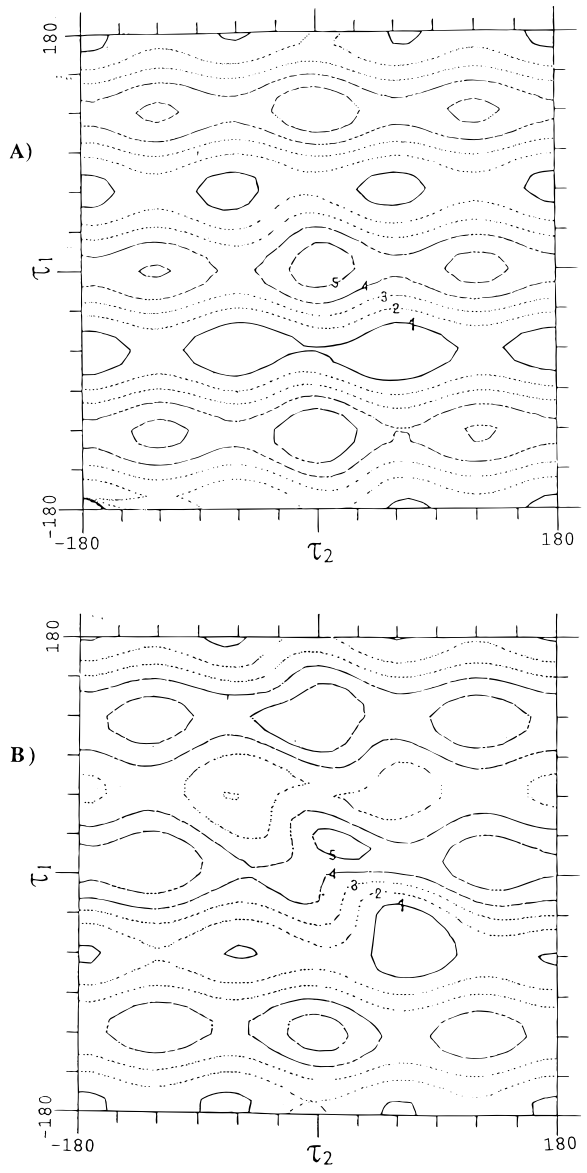

Figure 2. 2D contour maps displaying the potential energy of **5** (A) and **4** (B) as a function of torsion angles τ_1 (C15−C14−C17−O17) and τ_2 (C14−C17−O17−H17) at intervals of 10°. The numbered contours indicate relative energies at intervals of 1.18 kcal/mol for A and 1.26 kcal/mol for B.

torsion angles τ_1 (C15−C14−C17−O17) and τ_2 (C14−C17−O17−H17). These were calculated by relaxing the entire molecule while systematically sampling τ_1 and τ_2, with the torsional angles ϕ_1, ϕ_2, ϕ_3, and ϕ_4 predefined[7a] at the low-energy values determined by the one-bond drive calculations described above. The results show three minima, around −60°, 60°, and 180°, for the angles τ_1 and τ_2. The solid line contour at approximately $\tau_1 = -60°$, and $\tau_2 = 60°$ is the calculated minimum energy conformation, while the dash line contours at approximately $\tau_1 = -120°$ and $\tau_2 = 0°$ is the highest energy conformation. Three minimum conformation rotamers are possible by rotation around the C14−C17 bond of **5**, and the rotational energy barrier for the angle τ_1 of **5** was found to be 0.4 kcal mol^{-1}. None of the three conformations is compatible with an intramolecular H-bond between the hydroxymethyl group and the phenolic OH, a finding that is in agreement with our NMR results. Two refined conformations were obtained and are represented graphically in Figure 3 with the angle values listed in Table 1.

The same methodology was employed to investigate the orientation of the hydroxymethyl group in **4** (Figure 2). The minimum energy conformation occurs when $\phi_1 = -115°$ (i.e. when Ph-OH is directed towards the β face of the cyclohexyl rings), $\tau_1 = -30°$ and $\tau_2 = 60°$, which allows formation of an intramolecular H-bond between the hydroxymethyl OH as the donor and phenolic hydroxyl OH as the acceptor. At the minimum energy point, the H-bonding distance is 2.03 Å (159°). Thus, based on the computational data, this conformation of **4** is preferred due to stabilization through the intramolecular H-bond. This conformer was retrieved from the recorded file through the trajectory animation option, and subjected to further energy minimizations without any constraint. The results of these refined conformations for **4** are given in Table 1. Two of these low-energy conformers, one of which involves H-bonding between the Ph-OH and the southern OH, are graphically shown in Figure 3.

NMR Results. The 1D proton NMR spectra of **5** and **4** reflect the dynamic behavior of these molecules. The aromatic regions of the 1D ^{1}H spectra at low temperatures (Figure 4) show two sets of peaks that differ in intensity. Each set is comprised of two doublets and a singlet consistent with the aromatic spin system. In $CDCl_3$ the intensity of the major peaks compared to the minor is 1:0.3 for **4** and 1:0.15 for **5**. In DMSO the ratio of major to minor peak intensities is 1:0.15 for both **4** and **5**. The two sets of peaks are characteristic of slow exchange on the chemical shift time scale, between two unequally populated orientations of the phenol ring relative to the cyclohexyl ring system. This is evidenced by exchange cross peaks between the two sets of peaks observed in NOESY spectra (discussed below) and by the spectral changes that occur with increasing temperature.

Figure 5 shows spectra of **4**, focusing on the aromatic region, acquired in $CDCl_3$, and at increasing temperatures. The peaks broaden and change in chemical shift so that between 303 and 313 K, complex line shapes are observed that are characteristic of intermediate exchange. These spectra indicate an increase in the rate at which nuclei are exchanging between sites. At 323 K there is only one set of peaks visible. Beyond this coalescence point, the spectra are characteristic of fast exchange on the chemical shift time scale. The peaks sharpen indicating an increase in the rate of exchange between the two conformations so that there is averaging between the two sets of peaks. The assignment of resonances is discussed below.

Thermodynamic parameters for rotation around the C6−C7 bond at the coalescence temperature were derived on the basis of the major and minor resonances of the H2 proton as it was not involved in coupling. The calculation required the chemical shift difference between the major (M) and minor (m) H2 resonances and the population difference between the two conformations as determined from the low temperature spectra.[20,21] At 323 K, the difference in free energy (ΔG) between the two states in the case of **4** was 0.8 kcal/mol with $\Delta G^{\ddagger}_{M\rightarrow m} = 16.9$ kcal/mol and $\Delta G^{\ddagger}_{m\rightarrow M} = 16.1$ kcal/mol. The lifetime of the major conformer was 38.7 ms and that

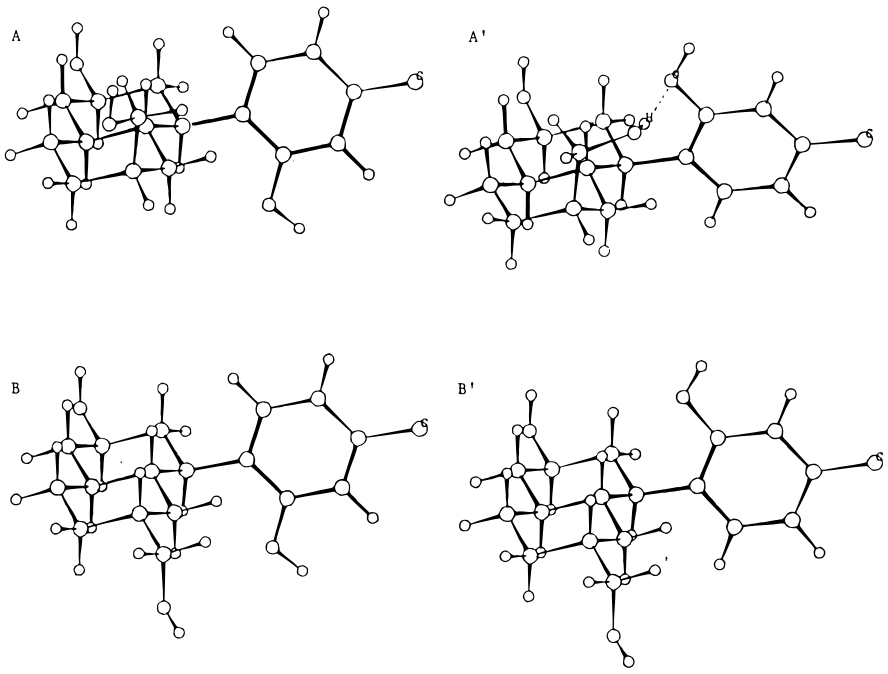

Figure 3. Graphic representations of the energetically preferred conformations of **4** (A and A′) and **5** (B and B′). (The DMH side chain is not displayed.)

Table 1. Structural Features and Relative Energies of Conformations of **4** and **5** as a Function of Torsional Angles (τ_1, τ_2) Calculated by Using Dihedral Drive Techniques and Later by Retrieving the Conformations for Further Energy Minimization until the Maximum Derivative Is Less Than 0.001 kcal/mol

compd[a]	relative energy (kcal/mol)	dihedral angle[b] ϕ_1	ϕ_2	τ_1	τ_2	H-bonding X−H···Y[c] (Å)	X···H−Y[d] (Å)
4A	9.25	62	0.5	−174	180		
4	9.99	−115	0.4	−175	−180		
4A′	8.09	−101	1.6	−41	67	2.03 (159°)	3.06 (63°)
5B	8.08	63	0.2	−61	179		
5B′	8.71	−116	0.8	−59	180		

[a] The letters **A**, **A′**, **B**, and **B′** indicate the corresponding conformations that are represented graphically in Figure 3. [b] ϕ_1 and ϕ_2, are defined as the dihedral angles C5−C6−C7−C8 and C2−C1−O−H, respectively. τ_1 and τ_2 are defined as the dihedral angles C15−C14−C17−O17 and C14−C17−O17−H17, respectively. [c] X−H···Y represents the H-bond distance between the proton of the hydroxymethyl 17-OH (H, as donor) and oxygen of the phenolic OH group (O, as acceptor). The value in parentheses is the angle of the H-bond X−H···Y. [d] X···H−Y represents the H-bonding distance between the oxygen of the hydroxymethyl 17-OH (O, as acceptor) and the proton of phenolic OH group (H, as donor). The value in parentheses is the angle of the H-bond X···H−Y.

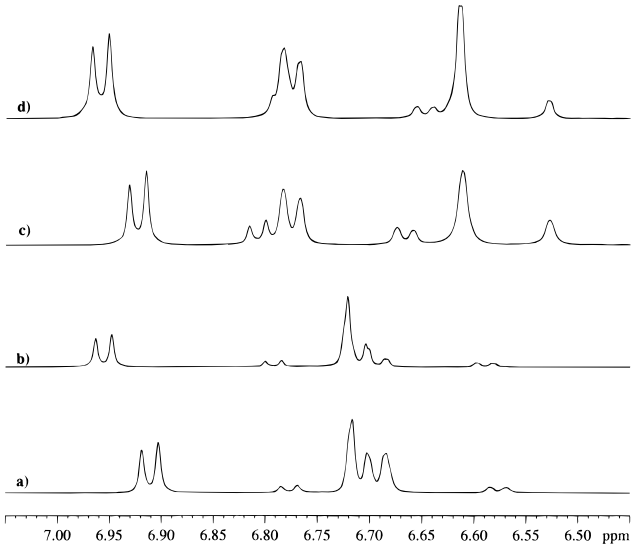

Figure 4. Aromatic 1D ^{1}H spectral regions of (a) compound **4** acquired at 298 K in DMSO, (b) compound **5** acquired at 298 K in DMSO, (c) compound **4** acquired at 263 K in $CDCl_3$, and (d) compound **5** acquired at 263 K in $CDCl_3$.

of the minor conformer was 11.5 ms. In the case of **5**, ΔG = 1.2 kcal/mol, $\Delta G^{\ddagger}_{M\rightarrow m}$ = 17.2 kcal/mol, and $\Delta G^{\ddagger}_{m\rightarrow M}$ = 16.0 kcal/mol. The lifetimes of the major and minor conformers were 73.1 and 10.9 ms, respectively.

Assignment of Major Resonances. Resonances at 3.81 and 2.78 ppm in the spectrum of **5** were tentatively assigned as H9a and H7a, respectively, by comparison with the spectrum of **2**[7a] and were used as a starting point for analysis of the cyclohexyl coupling networks in the DQFCOSY spectrum. These protons couple through a vicinal mechanism to H16a, H8a, H8e, H10a, and H10e. The axial hydrogen H14a was identified by its vicinal coupling to the methylene hydrogens of the C17 hydroxymethyl group. The H14a proton shows coupling to H15a and H13a and the coupling network then extends to H16a, H12a, H15e, H13e, H12e, etc., thus allowing assignment of all aliphatic ring protons. Similarly, the proton resonances of the phenol ring and 1′,1′-dimethylheptyl side chain (DMH) were initially assigned by comparison with those of **2**[7a] and confirmed by the COSY spectrum. Heteronuclear ^{1}H−^{13}C (HMQC) experiments were employed to assign ^{13}C resonances and to confirm ambiguous ^{1}H assignments. The phenolic and aliphatic hydroxyl hydrogens were tentatively assigned by analogy with earlier analyzed spectra of other nonclassical cannabinoids[7a,b] and later confirmed by 2D ^{1}H chemical exchange experiments.

A similar strategy was used for the assignment of **4**. The ^{1}H NMR chemical shift assignments were tentatively made by comparison with the assignments for **5**

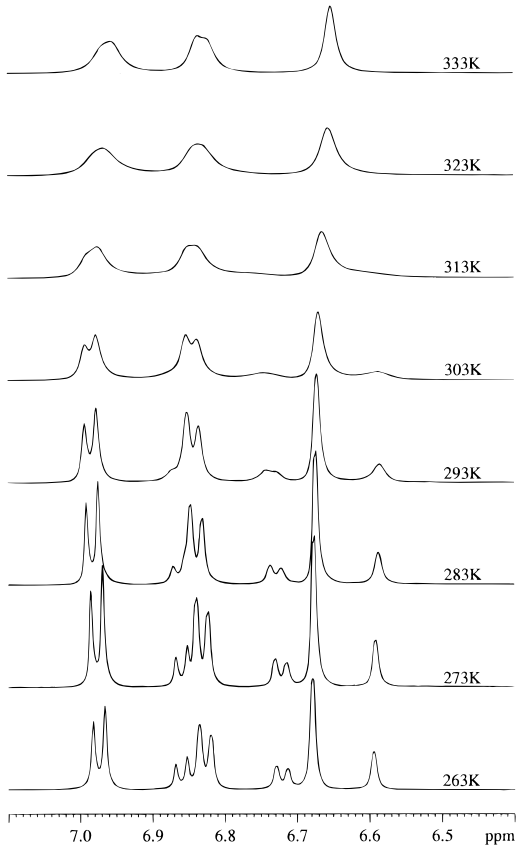

Figure 5. The aromatic 1D ^{1}H spectral regions of **4** in $CDCl_3$ acquired at 10° intervals.

and were confirmed by the DQFCOSY spectrum. Ambiguous assignments were further confirmed and ^{13}C resonances assigned by the ^{1}H−^{13}C HMQC spectrum. The resonance assignments for each diastereomer in $CDCl_3$ are summarized in Table 2.

A number of differences in the chemical shift of resonances between the two diastereoisomers were detected. Differences in the chemical shift of 12-CH_2, 13-CH_2, 14-CH_2, and 15-CH_2 were attributed to the axial versus equatorial position of the hydroxymethyl groups, which led to upfield or downfield shifting of these resonances in the diastereoisomer. For example, H13a (0.98 ppm) and H15a (0.56 ppm) resonances are shifted upfield for **5** in comparison with those of **4** (1.26 and 1.04 ppm, respectively). This is interpreted as a shielding effect from the C17−O σ-bond. The ^{13}C upfield shifts of 12-CH_2 (26.38 ppm), 16-CH (41.29 ppm), and 17-CH_2 (63.93 ppm) for **4** are credited as a γ-effect.

Minor Peak Assignment. Partial assignment of the minor peaks was possible based on the major peak assignments and exchange crosspeaks observed in NOESY spectra (Figure 6). Downfield resonances were easily assigned in this way however the resonances in the upfield region could not be detected due to overlap. The aromatic resonances H2, H4, and H5 show large chemical shift differences between major and minor resonances due to different orientations of the phenol around the C6−C7 bond. The H7 resonance on the cyclohexyl ring shows a particularly large chemical shift difference between the major peak and minor peak. The downfield chemical shift of the major peak compared to the minor peak is possibly due to the close proximity of the phenol oxygen in the case of the major conformer.

Table 2. ^{1}H NMR at 500 MHz and ^{13}C NMR at 125 MHz Chemical Shift Assignments

compound 4			compound **5**		
hydrogen	^{1}H (δ, ppm)	^{13}C (δ, ppm)	hydrogen	^{1}H (δ, ppm)	^{13}C (δ, ppm)
2	6.67	113.06	2	6.67	112.97
4	6.83	118.79	4	6.85	118.84
5	6.98	126.24	5	7.03	126.60
7a	2.74	39.00	7a	2.78	38.86
8e	2.09	43.52	8e	2.07	43.70
8a	1.40	43.52	8a	1.43	43.70
9a	3.81	70.42	9a	3.81	70.34
10e	1.98	42.93	10e	2.01	43.00
10a	1.17	43.93	10a	1.17	43.00
11a	1.17	40.94	11a	1.18	41.03
12e	1.77	26.38	12e	1.76	33.34
12a	1.48	26.38	12a	1.16	33.34
13e	1.51	28.83	13e	1.80	29.31
13a	1.26	28.83	13a	0.98	29.31
14a	1.86	36.04	14e	1.42	40.66
15e	1.45	30.90	15e	1.47	32.77
15a	1.04	30.90	15a	0.56	32.77
16a	1.17	41.29	16a	1.14	46.39
17a	3.62	63.93	17a	3.35	68.54
17b	3.51	63.93	17b	3.34	68.54
2′	1.53	44.64	2′	1.53	44.76
3′	1.04	24.54	3′	1.05	24.59
4′	1.17	30.17	4′	1.18	30.08
5′	1.18	31.81	5′	1.19	31.90
6′	1.22	22.68	6′	1.22	22.72
7′	0.84	14.11	7′	0.84	14.14
8′,9′	1.23	28.77	8′,9′	1.23	28.69
1-OH	4.85		1-OH	4.85	
9-OH	1.70		9-OH	1.70	
17-OH	1.32		17-OH	1.69	

In contrast the H9a and H17 resonances that are located further away from the phenol do not exhibit a large chemical shift difference between the two orientations of the phenol.

Determination of Coupling Constants. The ^2J and ^3J values were approximately determined by first-order analysis[14] of the individual multiplets obtained as F2 cross section spectra from the 2D phase-sensitive COSY spectra. The approximate J values and the chemical shift values were then used as a starting point for iterative simulation of the subspectra using Bruker's LAOCOON-based PANIC computer program as described by us in earlier publications.[7a,b,14] This iterative simulation process allowed the determination of the selected geminal and vicinal coupling constants between the aliphatic hydrogens of the cyclohexyl ring and the 17-CH_2OH group. The results of the simulation are listed in Table 3.

NOE Measurements. Cross peaks opposite in sign to chemical exchange crosspeaks were observed in NOESY spectra that were due to intramolecular NOEs. The significance of specific NOE interactions in determining the three dimensional geometry of **4** and **5** is detailed in the following Discussion section. The NOE dipole−dipole interactions obtained by the NOESY spectrum were confirmed by carrying out 2D ROESY NMR experiments which gave similar results. Except where noted, the spatial information provided by this experiment for the comparison of the diastereomers is the same as that for the 2D NOESY experiments.

Discussion

In this section, the similarities and differences between **4** and **5** are discussed with regard to (i) the

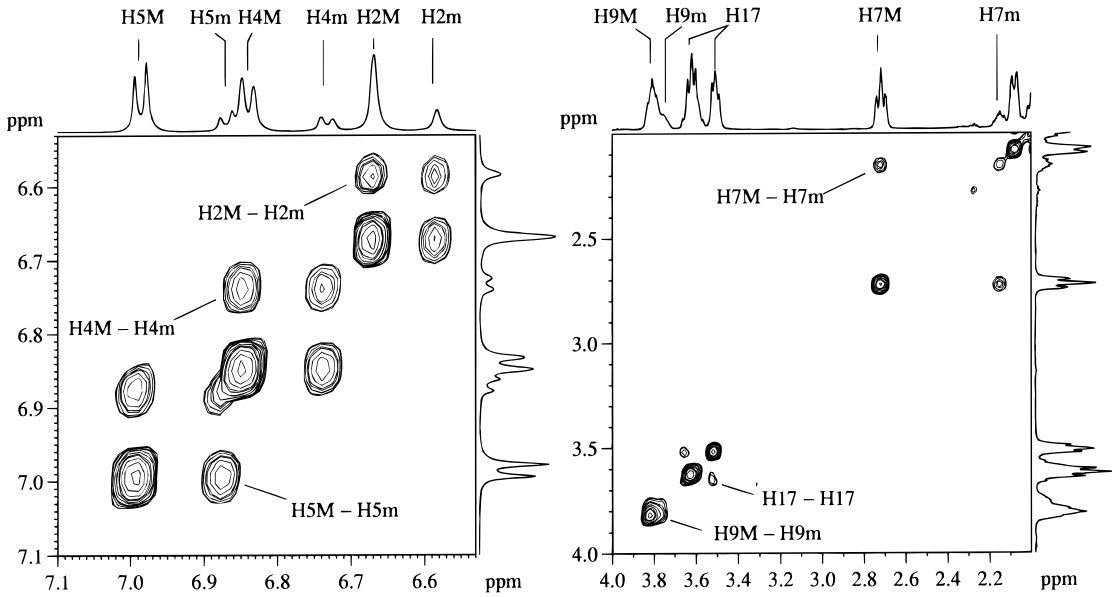

Figure 6. Two regions of a 100 ms NOESY showing exchange cross peaks between the major and minor peaks in the spectrum.

Table 3. Coupling Constants Determined by Iterative Simulation of the Subspectra Using Bruker's PANIC Program and Calculated Dihedral Angles

	compound **4**			compound **5**		
type of coupling	H′:H	coupling constant ^nJ value[a] (Hz)	dihedral angle[b] (deg)	H′:H	coupling constant ^nJ value[a] (Hz)	dihedral angle[b] (deg)
geminal ^2J	8a−8e	−12.3	*c*	8a−8e	−12.5	*c*
	10a−10e	−12.6	*c*	10a−10e	−12.6	*c*
	17a−17b	9.9	*c*	17a−17b	12.4	*c*
vicinal ^3J	7a−8a	10.8	158	7a−8a	10.8	158
	7a−8e	4.0	58	7a−8e	4.1	57
	7a−12a	11.7	161	7a−16a	11.5	160
	8a−9a	10.8	158	8a−9a	10.8	158
	8e−9a	4.3	57	8e−9a	4.3	57
	9a−10a	10.7	158	9a−10a	10.9	159
	9a−10e	4.2	56	9a−10e	4.2	56
	17a−14e	8.7	*d*	17a−14a	5.8	*d*
	17b−14e	7.6	*d*	17b−14a	5.8	*d*
	17a−HO	1.0	*d*	17a−HO		*d*
	17b−HO	6.9	*d*	17b−HO		*d*

[a] Obtained from 1D or 2D experimental spectra and refined through spectral simulation using PANIC; *n* is the number of bonds through which coupling occurs: geminal, $n = 2$; vicinal, $n = 3$. [b] Calculated using the equation $^3J = K \cos^2 \phi$; where $K_{a-a} = 12.5$ Hz, $K_{a-e} = K_{e-a} = 14.3$ Hz, and $K_{e-e} = 12.9$; ϕ is the dihedral angle, *K* values calculated from 1,3,5-trimethylcyclohexane.[15] [c] Geminal bond angles cannot be quantitatively determined. [d] Vicinal bond angles cannot be quantitatively determined. The couplings between H17ab and OH were not observed for **5**.

conformation of the 1′,1′-dimethylheptyl side chain, (ii) the conformation of the decalin (C ring) system, (iii) the orientation of the aromatic ring (A ring) relative to the C ring, and (iv) the orientation of the hydroxymethyl group as well as the formation of an intramolecular H-bond.

Conformation of the 1′,1′-Dimethylheptyl Side Chain. The 100 ms NOESY results of **5** show that NOE interactions of similar magnitude are observed between the 8′- and 9′-methyl protons (1.23 ppm) and the aromatic H2 (6.67 ppm) and H4 (6.85 ppm) protons. In addition, NOEs are also observed between the 2′-CH_2 hydrogens (1.53 ppm) and the H2 and H4 phenolic ring hydrogens. The 100 ms NOESY spectrum of the other diastereoisomer, **4**, shows similar NOE effects for the 8′- and 9′-CH_3 and 2′-CH_2 protons with the aromatic H2 and H4 protons. These data suggest that in both molecules the preferred conformations for the 1′,1′-dimethylheptyl side chain have the side chain almost perpendicular to the plane of phenol ring (Figure 7) and ϕ_3 (C2−C3−C1′−C2′) is approximately 60° or 120°. The NOE patterns allow for the possibility of four dynamically averaged conformations on the NMR time scale, a finding that is consistent with the results obtained for **2**.[7a]

The experimentally determined conformations are congruent with the computational model. A conformational search for the DMH chain showed four almost equienergetic conformers differing from each other by no more than 0.4 kcal/mol, while rotation of the DMH side chain around ϕ_3 and ϕ_4 (C3−C1′−C2′−C3′) shows energy barriers of 7.5 and 8.0 kcal mol^{-1} for **4** and **5**, respectively.

Conformation of the *trans*-Decalin Rings. As expected, the *trans*-decalin ring systems for both **4** and **5** appear to exist in chair conformations with no apparent distortions. Direct evidence for such an analysis is provided by vicinal coupling constants (Table 2) from which dihedral angles are calculated. Additionally, the observed NOE interactions between axial protons are

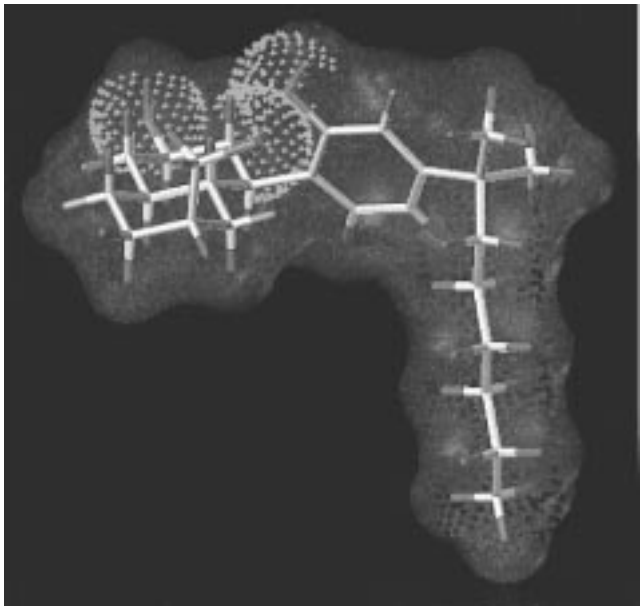

Figure 7. The biologically active conformation of **4**. The water-accessible surface area of the molecule is shown in green. The hydrophilic "head" portion of the molecule is highlighted by red dots and the hydrophobic "tail" is shown in blue.

consistent with such an analysis. For example, H9a (3.82 ppm) of **5** has dipolar interactions with both H7a (2.79 ppm) and H11a (1.01 ppm) of approximately equal magnitude, as does H15a (0.56 ppm) with H11a (1.18 ppm) and H13a (0.98 ppm).

Orientation of the A ring with Respect to the C Ring. The 100 ms NOESY spectrum for **5** shows NOE cross peaks between the major peaks of the aromatic H5 hydrogen (7.03 ppm) and the decalin protons, H8a (1.43 ppm) and H16a (1.14 ppm). Thus the major conformer is such that the H5 proton is oriented toward the β face of the cyclohexyl ring system ($\phi_1 = 63°$). Cross peaks between the minor peaks are not observed at short mixing times. At longer mixing times (500 ms), a weak NOE is observed between the minor peaks H7a and H5. This NOE taken together with the observation that major H7a resonance is downfield of the minor H7a resonance (Figure 5) suggests that the minor conformation is such that the H5 is facing the α-face of the cyclohexyl ring system ($\phi_1 = -116°$).

The 100 ms NOESY spectrum of **4** shows NOE cross peaks due to the interactions of H5 (6.98 ppm) with H16a (1.17 ppm), H8a (1.40 ppm), and H7a (2.74 ppm) that are similar to those of **5**, indicating the existence of the two conformers around the C6−C7 bond. However in this case the minor conformer is twice as populated as the corresponding conformation of **5** as shown by the intensity of the minor peaks compared to the major peaks (Figure 4). This is attributed to the fact that, for the minor conformer of **4** ($\phi_1 = -115°$), the axial CH_2OH is in position to form a H-bond with Ph-OH, while the equatorial methoxy group of **5** cannot form such a bond. This is supported by the decrease in the minor conformer population of **4** when dissolved in DMSO. This more polar solvent disrupts the intramolecular hydrogen bonding, leading to a decrease in this population.

The correlation between the A and C ring conformation and H-bonding in **4** is well-supported by the results of our molecular modeling study shown in Table 1. The dihedral drive calculations of the two-ring systems showed two energy minima separated by relatively large rotational energy barriers (20.5 kcal/mol for **4** and 21.2 for **5**). The magnitude of these calculated energy barriers is in agreement with the experimental results. Such a high-energy barrier can be attributed to unfavorable 1,6-interactions between the 15-CH_2 and Ph-OH. The calculated energy barrier for either of the two diastereoisomers is higher than for the prototype molecule **2** (the energy barrier of the C6−C7 bond for **2** is 9.1 kcal mol^{-1}).[7a] This indicates that the van der Waals repulsive interaction between 15-CH_2 and 1-OH for these diastereoisomers is much stronger than the corresponding 12-CH_2/1-OH interaction for **2**. The calculated energy (Table 1) shows that the conformer of **5** with $\phi_1 = 63°$ is favored. This is also the case for **4**, unless the proton of the 17-OH is in position to hydrogen bond with the phenolic OH group when the later is located on the β-face of the decalin ring system (Table 1).

Conformational Properties of the Hydroxymethyl Group. The rotational energy barrier about τ_1 (C15−C14−C17−O17) for **4** and **5** was calculated to be 4.5 and 4.0 kcal mol^{-1}, respectively (comparable to 6.7 kcal/mol for butane under the same condition). Such a barrier would not prevent free bond rotation. Molecular modeling results using the two-bond driver technique (Figure 2) are consistent with the experimental results and suggest a possible intramolecular H-bond in **4** between the southern OH and Ph-OH. Systematically rotating the dihedral angles τ_1 and τ_2 of **4** at intervals of 10° with the other torsional angles predefined[7a] at $\phi_1 = -115°$, $\phi_2 = 0.4°$, $\phi_3 = -56°$, and $\phi_4 = -56°$, reveals a minimum energy conformation with $\tau_1 = 152°$ ($\phi_1 = -112°$, $\phi_2 = -6.5°$, $\phi_3 = -40°$, and $\phi_4 = 70°$) and an intramolecular H-bond distance of 2.54 Å between the southern OH and Ph-OH. This conformer was then subjected to further minimization without any restraint on the torsional angles resulting in the torsion angles shown in Table 3 and a H-bonding distance of 2.03 Å (159°). Figure 3A′ shows a conformer of **4** with an intramolecular H-bond between the proton of 17-OH (as the donor) and the oxygen of the phenolic hydroxyl OH (as the acceptor). Such an intramolecular H-bond stabilizes the conformation of **4** with the phenolic hydroxyl group directed toward the β face ($\phi_1 = -101°$). The same method, used to study the orientation of the hydroxymethyl group of **5**, provided no evidence of an intramolecular H-bond. The preferred conformation of **5** is graphically represented by conformer **B** in Figure 3, and numerically represented by the angle values in Table 3. The phenolic OH in this molecule prefers to point down toward the α face ($\phi_1 = 63°$).

Conclusion

The preferred conformations for two nonclassical cannabinoid diastereoisomers, **4** and **5**, were determined using NMR techniques and computer modeling. The A and C rings are almost perpendicular to each other ($\phi_1 = 63°$ or $-110°$), the proton of the Ph-OH moiety is pointing away from the cyclohexyl ring and *syn* to H2 (Figure 3), and the dimethylheptyl side chain randomly adopts one of four equivalent minimum energy conform-

ers (i.e., $\phi_3 = -56°$ and $\phi_4 = -57°$). Although the only structural difference between these two molecules lies at the chiral center at C14, their conformations differ in two major aspects. One difference involves the relative orientation of the phenol ring (A ring) with respect to the fused decalin ring system (C and D rings). The A ring of **5** prefers the orientation with the Ph-OH directed toward and α face of the decalin ring system (Figure 3B). The A ring of its more biologically active diastereomer **4** shows an increased preference for the conformation in which the Ph-OH is directed toward the β face of the decalin ring system (Figure 3A′), suggesting that this may be the more biologically preferred conformation (Figure 7). This conformation of **4** is stabilized by an intramolecular H-bond. The hydrogen bonding between Ph-OH and 17α-OH does not occur in the less active diastereomer, **5**.

The conformational differences between these two diastereoisomers may be correlated to their biological activities and may explain the observed differences in their analgesic effects as nonclassical cannabinoids. The biologically preferred conformer of **4** has the 9β-OH, 17β-OH, and Ph-OH located on the same face of the two ring systems, thus giving this conformation an amphipathic nature in a manner similar to the conformer adopted by the parent compound **3**[7b] (Figure 7). Hence we can postulate that this conformation is also favored within a biological membrane medium, where the polar side of the molecule interacts with the hydrophilic region of the bilayer, while the hydrophobic side, which includes the DMH side chain, interacts with the hydrophobic region of the membrane. According to this argument, the greater ability of **4** to adopt this conformation allows it to be incorporated into biological membranes more easily than **5**. It is also possible that **4** is better able to assume an orientation within the membrane bilayer which allows it to diffuse laterally and interact favorably with the receptor active site.[2,7b]

In a similar fashion, the increased potency and selectivity of **4** compared to its precursor, **3**, may be attributed to the more defined stereochemical properties of this tricyclic analog. Indeed, the formation of a third ring in the case of **4** causes the 14-hydroxymethyl group to be spatially restricted to the β face of the rings as opposed to the flexible 12-hydroxypropyl group of **3**. This presumably allows **4** to more easily assume an amphipathic conformation that is better incorporated in the membrane and is more complementary to the receptor site.

Acknowledgment. This work was supported by grants from the National Institute on Drug Abuse (DA-3801, DA-07215, and DA-00152). We acknowledge Pfizer for providing the analogs discussed in this paper and for providing assistance with the molecular modeling package. We would also like to thank Dr. Lawrence Melvin for fruitful discussions.

References

(1) Gaoni, Y.; Mechoulam, R. Isolation structure, and partial synthesis of an active constituent of Hashish. *J. Am. Chem. Soc.* **1964**, *86*, 1646.
(2) Makriyannis, A.; Rapaka, R. S. The Molecular Basis of Cannabinoid Activity. *Life Sci.* **1990**, *47*, 2173−2184.
(3) Melvin, L. S.; Johnson, M. R.; Harbert, C. A.; Milne, G. M.; Weissman, A. A Cannabinoid Derived Prototypical Analygesic. *J. Med. Chem.* **1984**, *27*, 67−71.
(4) Johnson, M. R.; Althuis, T. H.; Bindra, J. S.; Harbert, C. A.; Melvin, L. S.; Milne, G. M. *NIDA Res. Monogr. Ser.* **1981**, *34*, 68.
(5) Wilson, R. S.; May, E. L.; Martin, B. R.; Dewey, W. K. 9-Nor-9β-Hydroxylhexahydrocannabinols. Synthesis, Some Behavioral and Analgesic Properties, and Comparison with tetrahydrocannbinols. *J. Med. Chem.* **1976**, *19*, 1165.
(6) Johnson, M. R.; Melvin, L. S. The Discovery of Nonclassical Cannabinoid Anagetics. In *Cannabinoids as Therapeutic Agents*; Mechoulam, R., Eds.; CRC Press: Boca Raton, FL, 1986; pp 121−146.
(7) (a) Xie, X. Q.; Yang, D. P.; Melvin, L. S.; Makriyannis, A. Conformational Analysis of the Prototype Nonclassical Cannabinoid CP-47,497, Using 2D NMR and Computer Molecular Modeling. *J. Med. Chem.* **1994**, *37*, 1418. (b) Xie, X. Q.; Melvin, L. S.; Makriyannis, A. The Conformational Properties of the Highly Selective Cannabinoid Receptor Ligand CP-55,940. *J. Biol. Chem.* **1996**, *271*, 10640.
(8) Howlett, A. C. Reverse Pharmacology Applied to the cannabinoid receptor. *Trends Pharmacol. Sci.* **1990**, *11*, 395−397.
(9) Howlett, A. C.; Johnson, M. R.; Melvin, L. S.; Milne, G. M. Nonclassical Cannabinoid Anagetics Inhibit Adenylate Cyclase: Development of a Cannabinoid Receptor Model. *Mol. Pharmacol.* **1991**, *33*, 429−436.
(10) Rance, M.; Sorensen, O. W.; Bodenhausen, G.; Wagner, G.; Ernst, R. R.; Wuthrich, K. Improved Spectral Resolution in COSY ^{1}H NMR Spectra of Proteins via Double Quantum Filtering. *Biochem. Biophys. Res. Commun.* **1983**, *117*, 479−485.
(11) Bax, A.; Lerner, L. Two-Dimensional Nuclear Magnetic Resonance Spectroscopy. *Science* **1986**, *232*, 960−967.
(12) Bax, A.; Davis, G. ROESY. *J. Magn. Reson.* **1985**, *63*, 207−213.
(13) Diehl, P.; Kellerhals, H.; Lustig, E. Computer assistance in the analysis of high-resolution NMR spectra. In *NMR: Basic Principles and Progress*; Diehl, P., Fluck, E., Kosfeld, R., Eds.; Springer-Verlag: New York, 1972; pp 1−96.
(14) Kriwacki, R. W.; Makriyannis, A. The Conformational Analysis of Δ^9- and Δ9,11-Tetrahydrocannbinols in Solution using High Resolution Nuclear Magnetic Resonance Spectroscopy. *Mol. Pharmacol.* **1989**, *35*, 495−503.
(15) Booth, H. Applications of hydrogen nuclear magnetic resonance spectroscopy to the conformational analysis of cyclic compounds. *Prog. NMR Spectrosc.* **1969**, *5*, 149−381.
(16) INSIGHTII/DISCOVER is a molecular modeling software package of Biosym Inc., Barnes Canyon Rd, San Diego, CA 92121.
(17) (a) Weiner, S. J.; Kollman, P. A.; Case, D. A.; Singh, U. C.; Ghio, C.; Algona, G.; Profeta, S., Jr.; Weiner, P. A New Force Field for Molecular Mechanical Simulation of Nucleic Acids and Proteins. *J. Am. Chem. Soc.* **1984**, *106*, 765−784. (b) Weiner, S. J.; Kollman, P. A.; Nguyen, D. T.; Case, D. A. An all atom force-field for Simulations of Proteins and Nucleic Acid. *J. Comput. Chem.* **1986**, *7*, 230−252.
(18) Dauber-Osguthorpe, P.; Roberts, V. A.; Osguthorpe, D. J.; Wolff, J.; Genest, M.; Hagaler, A. T. Structure and Energetics of Ligand Binding to Protins: E. Coli dihydrofolate reductase-trimethoprim, a drug-receptor system. *Proteins: Struct.*, Funct., Genet. **1988**, *4*, 31−47.
(19) Dewar, M. A.; Zoebisch, E. G.; Healy, E. F.; Stewart, J. P. *AM1*, A New General Purpose Quantum Mechanical Molecular Mode. *J. Am. Chem. Soc.* **1985**, *107*, 3902−3909.
(20) Sandström, J. *Dynamic NMR Spectroscopy*; Academic Press: London, 1982; pp 77−123.
(21) Shanan-Atidi, H.; Bar-Eli, K. H. A Convenient Method for Obtaining Free Energies of Activation by the Coalescence Temperature of an Unequal Doublet. *J. Phys. Chem.* **1970**, *74*, 961−963.

JM960410R